Molecular Crystals and Liquid Crystals Science and Technology. Section A. Molecular Crystals and Liquid Crystals

Publication details, including instructions for authors and subscription information:
http://www.tandfonline.com/loi/gmcl19

Transitions to Ordered Phases in Systems Containing Rodlike Particles: I. A New Continuum Monte Carlo Approach

Larry A. Chick [a] & Christopher Viney [b]

[a] Pacific Northwest Laboratory, Richland, WA, 99352

[b] Center for Bioengineering, University of Washington, Seattle, WA, 98195

Version of record first published: 24 Sep 2006.

To cite this article: Larry A. Chick & Christopher Viney (1993): Transitions to Ordered Phases in Systems Containing Rodlike Particles: I. A New Continuum Monte Carlo Approach, Molecular Crystals and Liquid Crystals Science and Technology. Section A. Molecular Crystals and Liquid Crystals, 226:1, 25-40

To link to this article: http://dx.doi.org/10.1080/10587259308028789

Mol. Cryst. Liq. Cryst., 1993, Vol. 226, pp. 25–40
Reprints available directly from the publisher
Photocopying permitted by license only

Printed in the United States of America

Transitions to Ordered Phases in Systems Containing Rodlike Particles: I. A New Continuum Monte Carlo Approach

LARRY A. CHICK

Pacific Northwest Laboratory, Richland, WA 99352

and

CHRISTOPHER VINEY

Center for Bioengineering, University of Washington, Seattle, WA 98195

(Received October 31,1991, 1992; in final form July 24, 1992)

A new continuous-placement Monte Carlo (CMC) approach was developed that measures the entropy of rodlike particle configurations having pre-set global orientation distributions. Entropies are measured through a range of concentrations, independently of whether these configurations represent equilibrium conditions. Rod concentrations, orientation distribution shapes, and order parameters that are expected to be present at equilibrium can then be determined by comparing free energy curves. The method was applied to two-dimensional, monodisperse, athermal systems and the results demonstrated that choice of the shape of the global orientation distribution in the anisotropic phase can result in shifting from a first-order to a continuous isotropic-to-nematic phase transition.

Keywords: athermal, axial ratio, combinatoric entropy, Monte Carlo, orientational entropy, rodlike particles

INTRODUCTION

It has been known for a century[1–5] that solutions containing rodlike particles undergo spontaneous separation into isotropic and anisotropic phases, as the rod concentration is increased. The anisotropic phases have intermediate order between the liquid and the solid state. We will limit our attention to the nematic phase, which has long-range orientational order, but no positional order.

Although Langmuir[6] attempted to explain and, more recently, Maier and Saupe[7] succeeded in explaining the isotropic-to-nematic (I-N) transition based on the attractive forces between the rodlike molecules, it is now widely accepted[8–12] that the phenomenon can be explained on the basis of hard-core repulsive forces (steric hinderance). This is not to imply that intermolecular attractive forces have no effect

on the behavior of real systems; rather, since the basic phenomenon can be explained in the simpler terms of steric hinderance alone, the attractive forces can then be treated as perturbations on the (athermal) model system.

Near mid-century, two distinct theoretical approaches were developed to explain the I-N transition on the basis of steric hinderance. Onsager[13] modeled the system as a (continuum) gas of long rods, expressing the state function as a two-term virial expansion on the density. Although his approach did predict the existence of the I-N transition based solely on excluded volume effects, omission of higher-order terms to achieve mathematical tractability prevented accuracy at high concentrations and for short rods. Flory,[14] on the other hand, developed a discrete lattice model that represents the rods as sequences of occupied lattice cells, with each sequence oriented parallel to a preferred domain axis. The free energy of the system was expressed in terms of the orientational and the combinatoric (positional) entropy, the latter derived from the probability of finding an occupiable vacancy within the system for a rod with given disorientation from the preferred domain axis.

These distinct theories appear to have spawned two branches of subsequent investigations, which can be roughly differentiated on the basis of their respective representations of the rodlike particle system. On the one hand, the branch rooted in Onsager's theory[12,15–38] generally maintains representation of the system as a *continuum*, with the rods allowed continuous orientational and positional freedom. On the other hand, the branch traceable to Flory's theory[8,9,39–61] generally persists in modelling the system as a lattice, with rod position and, to various degrees, rod orientation, variable in *discrete* increments. Obviously, such a sweeping generalization will be contradicted in specific cases. Nevertheless, this broad distinction will serve to focus attention on the main intent of this and the following two papers,[62,63] which is to address the limitations of the discrete lattice representation in modeling the continuum.

It is somewhat inconsonant to model phases that have limited or no positional order in terms of a discrete lattice, in which the lattice cells (possible sites of the monomers) themselves have strict positional order. It would seem that such an approach is more suitable for modeling crystalline phases. However, the lattice models are generally more amenable to the incorporation of the complexities of real rodlike molecule systems (flexibility, polydispersity, orientation-dependent attractive forces, etc.) because they are generally simpler in terms of computation.[44] Thus, the discrete lattice approaches are still actively evolving in the quest to understand liquid crystalline phase transitions; that is, to predict the critical concentrations at which the phase transitions occur, whether the transitions are first- or second-order, or continuous, and the arrangements of the rods before, during, and after their alignment. However, we have found only one published work[64] that seeks to address the problems that may be introduced by representing what are essentially liquid-like phases (in terms of positional order) in the context of discrete positional possibilities. Okamoto[64] ran dynamic Monte Carlo for two-dimensional systems of flexible, athermal polymers. He varied the lattice cell size and, apparently, tested continuous placement with bond angles restricted to 0 and $\pi/2$. He found "appreciable" differences in pressure and osmotic pressure between the

lattice and the continuum systems at high concentrations. However, he did not investigate the fundamental *reasons* for the differences.

In this paper, we discuss a continuum Monte Carlo (CMC) approach to directly measure the combinatoric entropy as realistic configurations of rods are built up to fill a pre-set orientation distribution. Phase diagrams are developed for athermal systems of monodisperse, rigid rods in two dimensions. In the following paper[62] the specific differences between discrete lattice and continuum representations are enumerated through comparisons of our CMC measurements with the predictions of the Flory-type[8,14] discrete lattice model. The final paper[63] explores the root causes of the inaccuracies of the discrete lattice model and discusses some of the perceived implications.

Our attention is restricted to athermal systems of monodisperse, rigid rods. We note here that these restrictions pertain not only to a simplification of liquid crystalline systems, but are likely to be rather accurate descriptions of macroscopic systems such as ceramic fibers, toothpicks, etc.[65] Intermediate scale systems may also be well represented provided that the hard-core nature is augmented by strongly repulsive forces; e.g. suspensions of lipid tubules.[66]

The CMC studies were all performed for two dimensional systems because of computer limitations and because details of the microstructure, such as short-range order are more easily visualized in two dimensions than in three. The fundamental problems that result from the two-dimensional discrete lattice model representation are expected to be analogous to the problems encountered in discrete lattice model representations of three-dimensional systems. In keeping with the approach devised by Flory, and to enable comparison of our results with those of Flory's lattice model, we impose a global orientation distribution on the anisotropic (aligned) phases that we study. The existence of true long-range orientational order in a two-dimensional system has itself been a subject for debate, with many[5,11,18,30,67–69] but not all[24] arguments being made against it. In the present case, where we do not take account of thermal fluctuations, the reality of long-range order is implicit. We shall see that this approach leads to some interesting observations on the relation between long- and short-range order.[63]

CALCULATION OF FREE ENERGIES AND DETERMINATION OF EQUILIBRIUM

Flory[8,14] determined equilibrium between isotropic and anisotropic phases by adjusting the rod concentration in each until equality was achieved for the requisite pairs of chemical potentials, one pair each for the rod and the solvent components. We chose to calculate equilibria using the free energies of the requisite phases, this method being more straightforward for computations based on the CMC technique.

Because we deal strictly with athermal systems, the reduced free energy is composed of the sum of the negative orientational and combinatoric entropies. The orientational entropy, S_o, is calculated directly from the imposed global orientation distribution. For the CMC approach, the combinatoric (positional) entropy, S_c, is determined through measurements of vacancy fractions. Free energies can then be

calculated as functions of rod concentration for each phase, and are uniquely defined by choice of the axial ratio and the orientation distribution.

The Orientational Entropy

Unlike Flory's treatment, our method allows calculation of the orientational entropy without reliance on the lattice representation; that is, we do not express the orientation distribution in terms of the numbers of sequences required to represent the rod in the lattice, but rather in terms of the continuously variable angular orientation. Details of the orientational entropy calculation are given elsewhere[70] and can be summarized as follows: The distribution of thermodynamically distinguishable orientations for the two-dimensional system is expressed in terms of the absolute angle between the rods and the preferred domain axis, ψ, which can vary from zero for a perfectly aligned rod to $\pi/2$ for a rod having maximum disorientation. The orientational entropy per rod, S_o/n_x, is calculated directly from the preset global orientation distribution using:

$$S_o/n_x = \ln Z_o/n_x = -\sum_{i=1}^{I} m_i \ln m_i \tag{1}$$

where S_o is the orientational entropy, Z_o is the orientational partition function, n_x is the number of rods, and m_i is the fraction of rods that have orientations falling within those of the i^{th} increment out of the I total increments into which the orientation distribution is partitioned. For the isotropic distribution, in which the m_i are equal, we obtain:

$$(S_o/n_x)_{\text{iso}} = \ln I \tag{2}$$

The choice of the number of increments used in the calculation, I, is arbitrary, *so long as all distributions are compared on the same basis*. Therefore, in order to reference S_o to the isotropic distribution, we group $\ln I$ with S_o, obtaining a normalized value of zero for the isotropic distribution:

$$(S_o/n_x - \ln I)_{\text{iso}} = 0 \tag{3}$$

Distributions with less than perfect disorder will then be assigned normalized orientational entropies that are less than zero. For example, consider an ordered phase having the two-dimensional analog of Flory's[14] original uniform orientational distribution; the ψ are uniformly distributed between zero and ψ^+, such that none exceed ψ^+. Integration of (1) for this uniform orientation distribution yields[70]:

$$(S_o/n_x - \ln I)_{\text{unif}} = \ln\left(\frac{2\psi^+}{\pi}\right) \tag{4}$$

which gives entropies that is less than zero for all ψ^+ less than $\pi/2$. S_o for other distribution shapes is most conveniently determined by numerical methods.

The Combinatoric Entropy From Continuum Monte Carlo

In this section we summarize the use of a new continuum Monte Carlo (CMC) method for measuring the fraction of available vacancies within an assemblage of rods. The CMC measurements give an alternate method of determining the combinatoric partition function and entropy. This allows calculations of phase equilibria that are totally independent of a discrete lattice model.

We refer to our numerical experimental method as a Monte Carlo technique in the sense that a random number generator is used to control specific events. Most of the numerical studies in the field that are classed as Monte Carlo investigations[11,30–35,62,71–74] are in effect "annealing" or "dynamic" schemes that a) begin with a set configuration of molecules, b) use random numbers to control shifts of the position and/or orientation of individual molecules, c) accept or reject each move on the basis of a set of criteria related to simple particle infringement (but that may incorporate more complex energetic interactions), and d) seek to arrive at the equilibrium configuration, which is signified by lack of continued change in state-determining parameters. These are very powerful techniques for determining local rod configurations over the entire range of concentrations; however, they are not generally used to impose global orientation distributions, and they cannot be used to investigate the free energies of configurations under non-equilibrium conditions. Therefore, the annealing approach is not well-suited for our purpose of direct comparison to the results of Flory's discrete lattice model.

Our CMC method for the determination of vacancy fractions in rod configurations is essentially like the "wandering test molecule" method that was, apparently, first proposed by Widom[75] in a discussion of hard sphere liquids. We start with a blank placement square that is scaled to have sides equivalent to five or more rod lengths. Rods are added one at a time, their orientations and positions determined by use of a random number generator (though the orientations are constrained to

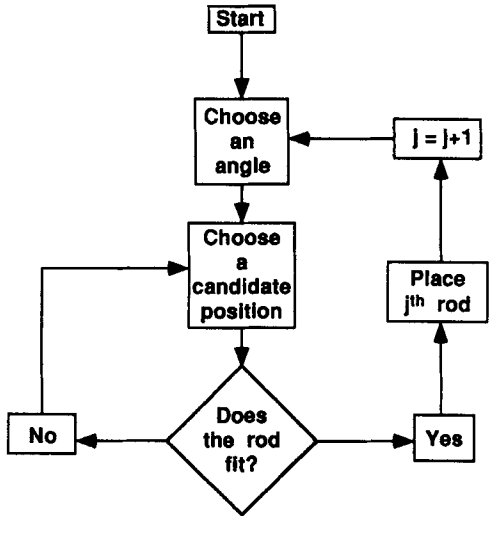

FIGURE 1 Flow chart for placement of rods by continuous Monte Carlo.

fill a pre-set distribution). The positions and orientations are continuously variable; that is, they are not restricted by discrete lattice cells. (Strictly speaking, the positions and orientations *are* selected on a discrete lattice because we are using a digital computer. However, the method approximates the continuum closely since the effective resolution of the lattice is typically 10^8 times finer than the length of the rods.) Periodic boundary conditions are used.[70] If a candidate rod is found to overlap an existing rod, then a new candidate position is generated at random; the process continues until the new rod is successfully placed, after which it is not allowed to move. The rod placement portion of the algorithm is diagrammed in Figure 1.

After a new rod has been placed, the rod placement portion of the algorithm pauses and the fraction of appropriate vacancies remaining in the configuration is measured by repeated attempts using test rods. These test rods are not actually placed within the configuration; they are used to measure vacancy fractions through determination of the fraction of test rods that do not impinge on existing rods on the first attempt at placement, P_j. The vacancy fraction measuring portion of the algorithm is diagrammed in Figure 2. Note that two adjustable parameters ("Have enough attempts been made?", and, "Have enough finds been scored?") are used to obtain adequate counting statistics. How these parameters were set is discussed below.

If j rods have been placed in the configuration and P_j is the fraction of test rods that do not impinge on existing rods during the subsequent vacancy-measuring stage, then we use[70]:

$$\frac{v_j}{K} = P_j \tag{5}$$

where v_j is the number of appropriate vacancies remaining within the configuration and K is the total number of ways originally available for placing rods within the (empty) system. The constant of proportionality, K, is a very large, undetermined number for systems like CMC that use continuous variability of rod position. For a discrete lattice, K is equal to the total number of lattice cells[70]. The ratio v_j/K is therefore the fraction of appropriate vacancies remaining after the j^{th} rod has been placed. In this manner, CMC is used to generate a measure of the fraction-of-vacancies as a function of rod concentration for the particular axial ratio and global orientation distribution being tested.

As we build up the assemblage, rods are placed with randomly chosen orientations that are constrained to eventually fill a pre-determined global orientation distribution. When we intend to measure the vacancies in an anisotropic phase, the orientations are constrained to the desired distribution from the beginning. Thus even when we have placed only a few rods, and the concentration is very low, those few rods tend to be aligned. On the other hand, when we intend to measure the vacancies in the isotropic phase, the rods are forced to remain randomly oriented even at high concentration. We are not attempting to mimic conditions of equilibrium at this stage of the procedure. At equilibrium, we expect low concentrations of rods to be randomly oriented (isotropic phase) and high concentrations of rods to be (imperfectly) aligned. However, using our CMC method, we

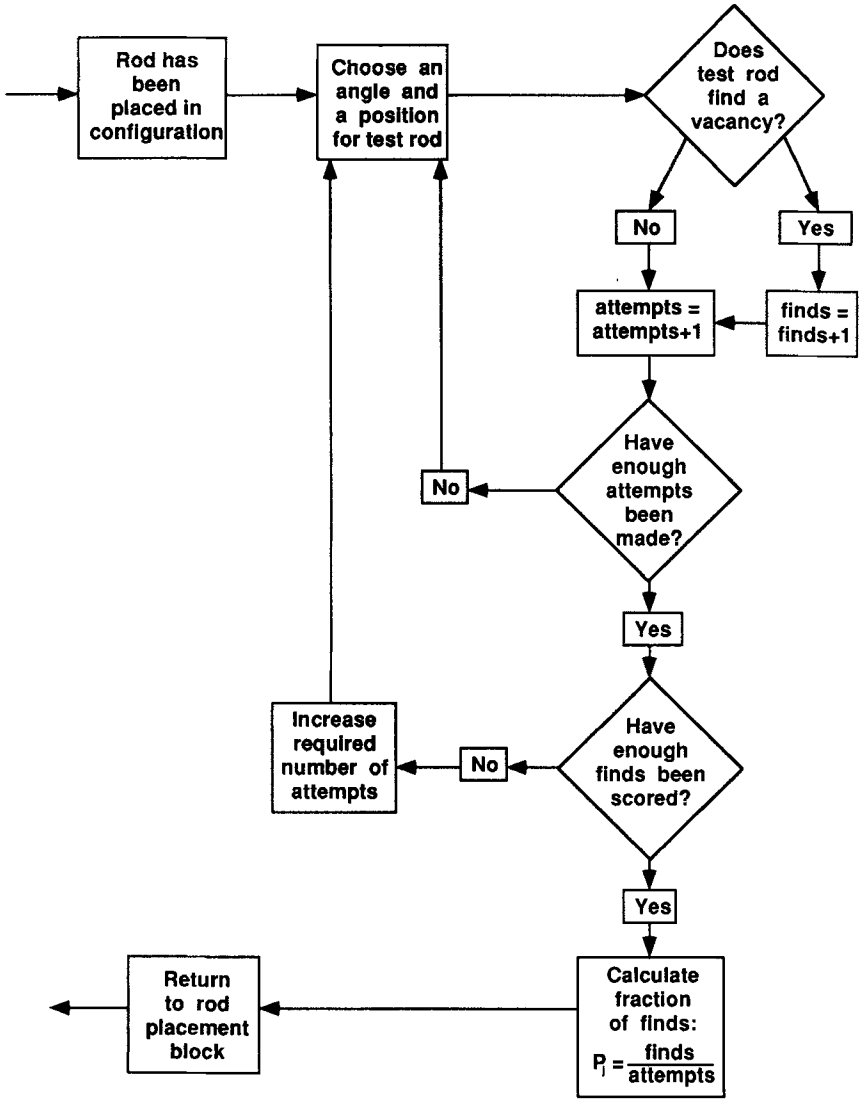

FIGURE 2 Vacancy fraction measuring portion of the Monte Carlo algorithm. This block fits between the "$j = j + 1$" and the "Choose an angle" operations of the rod placement block, which is shown in Figure 1.

cannot predict the state of the system at equilibrium without first knowing the free energies of the various possible orientation distributions through a range of concentrations. Thus we constrain the orientations to a predetermined distribution, build up the rod concentration—measuring the fraction of appropriate vacancies remaining as each new rod is added—and use this information to determine the free energy of this particular phase through the range of concentrations tested. Later we will compare the free energies of the various phases. Then we will find that, at equilibrium, a particular global orientation distribution is stable only within

a restricted range of concentrations, or at a single concentration or, possibly, not at any concentration.

Precision of the vacancy fraction measurements is improved by running the algorithm several times, with each run building up a new configuration, and averaging the fraction of finds data rod-by-rod over the several runs. Precision is also improved by requiring that a minimum number of finds are scored before the fraction of finds is calculated for the j^{th} rod within a particular run. If V is the number of runs and MS is the required minimum number of finds, then the precision should be proportional to the square root of MS*V, which was typically set to values in the range of 1000 to 3000.

Figure 3 shows CMC-generated vacancy fraction curves for isotropic and anisotropic configurations. The anisotropic configurations have normally distributed orientations of the form:

$$m_\psi \propto \exp(-(\psi/\sigma)^2/2) \tag{6}$$

where m_ψ is the fraction of rods having orientation, ψ, and σ is the standard deviation (controlling the width) of the normal distribution. Plots of three of these types of rod configuration are shown in Figures 4 to 6.

Third- to fifth-order polynomials are fit to the vacancy fraction curves[70] and the polynomials are used to calculate the combinatoric entropy, S_c, which is given by[8]:

$$S_c = \ln Z_c = -\ln(n_x!) + \sum_{j=1}^{n_x} \ln v_j \tag{7}$$

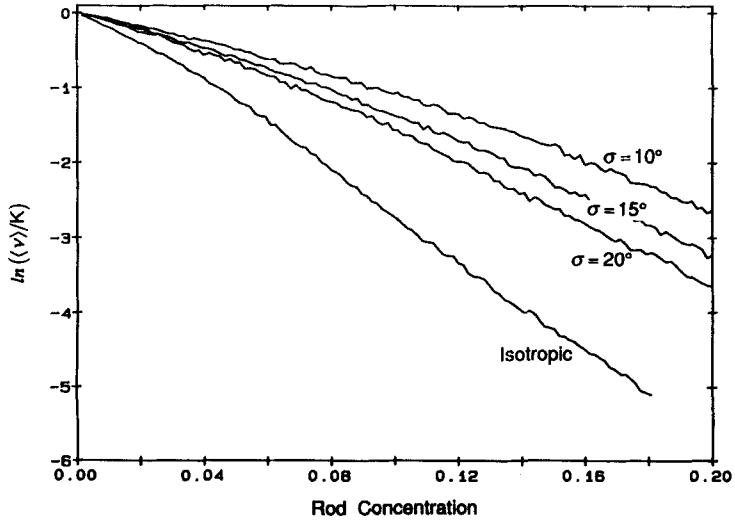

FIGURE 3 Logarithm fraction-of-vacancies for four orientation distributions. Precision of curve for the isotropic configuration is highest, with MS*V = 2400. Curves for configurations with normally distributed orientations have MS*V = 1000. The σ parameter controls the degree of order (standard deviation) in the configurations with normally distributed orientations. Rod axial ratio is 25, placement square is 5 rod-lengths on a side.

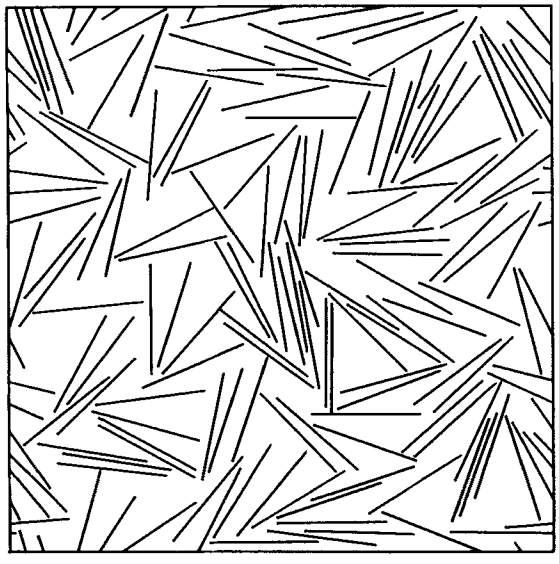

FIGURE 4 Isotropic configuration of rods with axial ratio of 25. Line-widths are not to scale. Rod concentration is 0.2384.

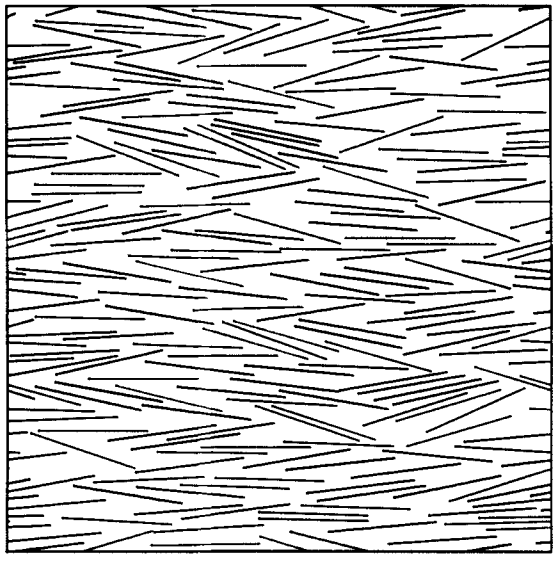

FIGURE 5 Configuration with normally distributed orientations (σ = 10°) imposed. Rod concentration is 0.336, axial ratio is 25.

where Z_c is the combinatoric partition function and n_x is the total number of rods having been placed. As discussed above, the CMC results actually yield v_f/K data (see Equation 5), where K is some very large, undetermined number (referenced to the empty system). The fact that K is not determined has no effect on the calculation of the *equilibrium* between phases because the fractions of vacancies

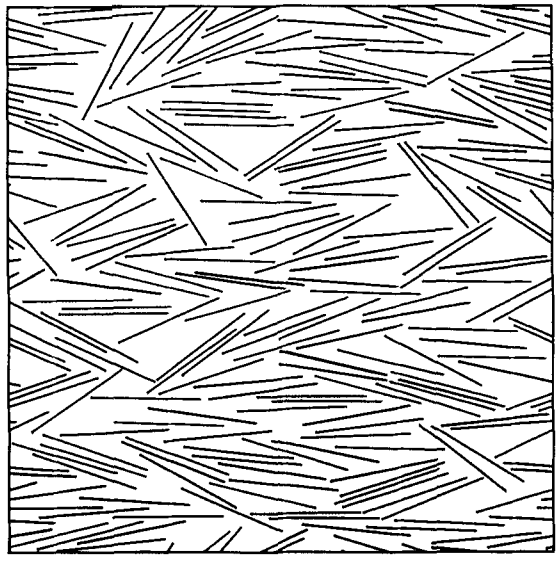

FIGURE 6 Configuration with normally distributed orientations ($\sigma = 20°$) imposed. Concentration and axial ratio are the same as in Figure 5.

in all phases are normalized by the same undetermined number. The choice of K is arbitrary since the effect is to subtract an identical linear function from all free energy curves, an operation that does not affect the relative positions or the relative slopes of the curves. The orientational entropy, S_o, is calculated from the preset global orientation distribution, using (1). As mentioned previously, for our athermal systems the free energy is simply the sum of S_c and S_o. [The reader may think of other statistical approaches to measuring combinatoric entropy. Refer to Reference 70, Appendix B for a more detailed discussion that draws attention to one alternative, but flawed, approach.]

Frenkel and Eppenga[30] used a similar "particle insertion" technique to measure the chemical potential of their dynamic Monte Carlo-generated configurations of infinitely thin rods. However, they apparently did not take orientational entropy into account, leading to questionable calculations of the chemical potential.

RESULTS

For our two-dimensional system with imposed long-range order in the anisotropic phase, the type of phase transition predicted depends upon the shape of the imposed orientational distribution. For rods having uniformly distributed orientations—the two-dimensional equivalent of Flory's original distribution[14,62] wherein allowed absolute disorientations are spread uniformly—a first-order transition (phase separation) is predicted between isotropic and anisotropic phases as the rod concentration is increased. In this case, a phase diagram containing a biphasic region is calculated. In the case of rods with normally distributed orientations—wherein the allowed disorientations are normally distributed around zero—a continuous tran-

sition is predicted, with the average degree of disorientation smoothly decreasing as the rod concentration is increased. In this case, no biphasic region is predicted; the results are presented in the form of a "phase evolution" diagram.

Results for Uniformly Distributed Orientations

Flory and Ronca[8] determined the volume fractions of the phases at equilibrium by requiring equality of the pair of chemical potentials for each of the components (rods and solvent molecules). Equality of the pairs of chemical potentials is certainly both a necessary and a sufficient condition for phase equilibrium, but its use in the derivation and computation of phase equilibrium overlooks a more straightforward method, that of finding the common tangent to the free energy curves. Common tangency also is both a necessary and a sufficient condition for phase equilibrium.[76] For systems in which the space is completely occupied by the combination of rods and isotropic solvent particles (as in Flory's construction, where each solvent molecule occupies one lattice cell), common tangency necessarily guarantees equality of the chemical potentials of both components.

Our computations of equilibrium are performed numerically but are based on the principles that are illustrated graphically in Gordon's treatment of the common tangent method.[76] Reduced free energy curves for an anisotropic and an isotropic phase are calculated as functions of the rod concentration. We find the tangent that is common to both free energy curves. The points of tangency give the rod concentrations in the respective phases under conditions of equilibrium. At lower concentrations the isotropic phase is stable; at higher concentrations the anisotropic phase is stable. At concentrations between the points of tangency, a two-phase mixture is stable. Within this biphasic region, the free energy of the system is given by the common tangent, not by the free energy curves.

We quantify the degree of disorder in the two-dimensional anisotropic phase by means of a simple order parameter, $\langle\psi\rangle$, defined as the average angle of rod orientation measured relative to the director. A larger value of $\langle\psi\rangle$ therefore denotes greater disorder.

In the case of an anisotropic phase orientation distribution shape that yields a first order I-N transition, it is necessary to determine the particular degree of disorder in the anisotropic phase within the biphasic region. This is done in the following manner: The common tangent is found between the free energy curve for the isotropic phase and each of several curves for anisotropic phases with different order parameters. A plot is made of the rod concentration needed for the anisotropic phase to form, as a function of the order parameter, as illustrated by the lower biphasic boundary in Figure 7. For a first-order transition, the minimum in the concentration of the lower biphasic boundary indicates the degree of disorder of the anisotropic phase which appears within the biphasic region. The particular order parameter corresponding to that minimum represents the first anisotropic phase to appear. The method is illustrated for anisotropic phases with uniform orientation distribution in Figure 7.

Figure 8 shows the results generated by CMC for axial ratios of 100, 40, and 25 with uniformly distributed orientations imposed; extension of the phase diagram for shorter rods becomes prohibitive due to rapidly increasing computer run times.

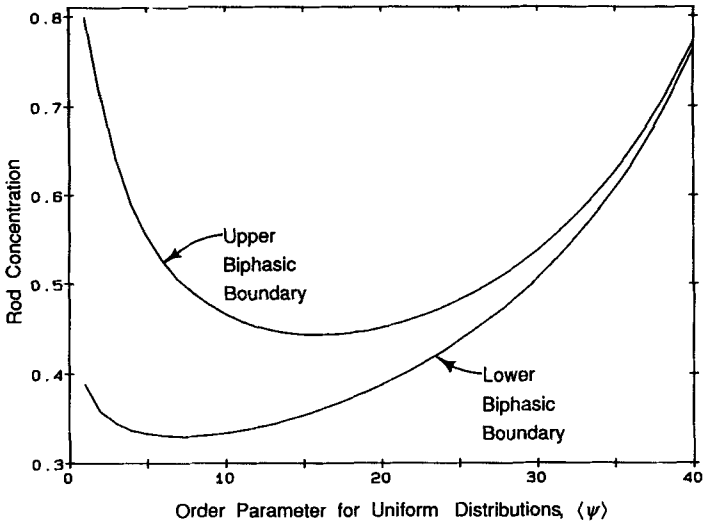

FIGURE 7 Typical biphasic boundary curves for systems that exhibit first order I-N transition. These data are for configurations with uniform orientation distributions imposed (axial ratio is 25), calculated here by the discrete lattice model,[62] though the same approach would pertain to data calculated by CMC. The minimum in the lower biphasic boundary curve indicates the degree of order in the anisotropic phase that is in equilibrium within the biphasic region. The average rod disorientation, ⟨ψ⟩, represents an order parameter.

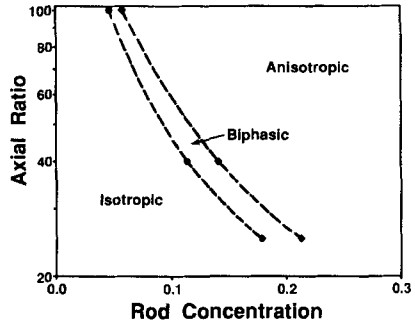

FIGURE 8 Portion of phase diagram for two-dimensional system of athermal, monodisperse rods with uniform orientation distributions imposed. These phase boundaries, generated using the continuous Monte Carlo (CMC) approach, inidicate a first-order I-N transition.

Results for Normally Distributed Orientations

In the case of normally distributed orientations, we use the standard deviation, σ, of the distribution as an order parameter for the anisotropic phase. Again, therefore, a larger value denotes greater disorder.

For anisotropic phase orientation distribution shapes that yield a continuous I-N transition, there will be no minimum in the curves for the biphasic boundaries, as shown in Figure 9. These results suggest a smooth evolution of increasing order as the rod concentration is increased. A map of the equilibrium degree of alignment as functions of axial ratio and rod concentration is obtained by determining the

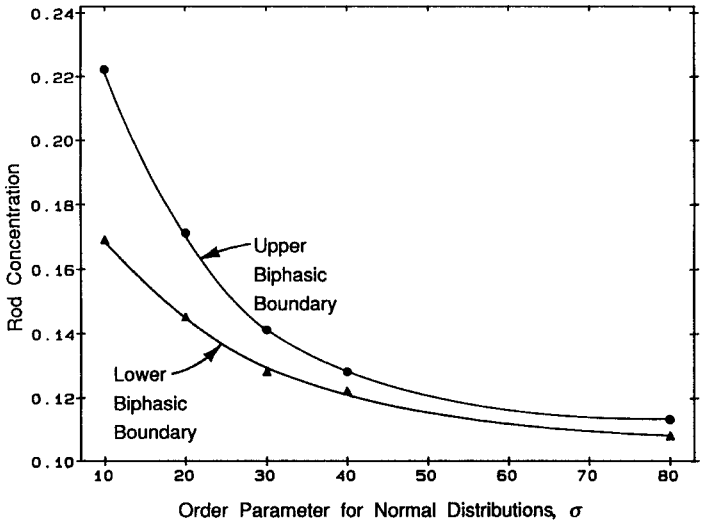

FIGURE 9 Attempt to identify the critical order parameter, σ, for the anisotropic configuration with normally distributed orientations imposed in the two-dimensional system with $x = 25$. The absence of a minimum in the curve for the lower biphasic boundary indicates this system exhibits a continuous phase transition; the degree of order increases continuously as the rod concentration is increased. Data points are from the CMC method. Lines are drawn to fit the data points.

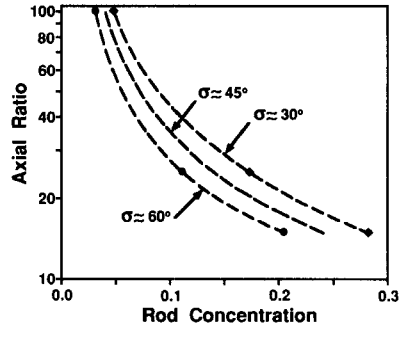

FIGURE 10 Portion of phase evolution diagram for two-dimensional system of athermal, monodisperse rods with normally distributed orientations imposed. These order parameter contours, generated using the continuous Monte Carlo (CMC) approach, indicate a continuous I-N transition.

concentration at which the free energies of two anisotropic phases with different order parameters are equal. We refer to the resulting plot of order parameter contours as a phase evolution diagram.

Figure 10 shows the phase evolution diagram generated by CMC for axial ratios of 100 through 15, with normally distributed orientations imposed. The contour for 60° was determined by finding the concentration at which the free energy for a phase with a standard deviation, σ, of 40° is equal to that of a phase with σ = 80°. Similarly, the contour for 30° represents equality of the free energies of phases with σ of 40° and 20°. The contours then indicate the concentrations where the distribution is expected to have a σ intermediate to those used in the calculation, and are labeled as such.

The phase diagram for uniform orientation distributions is compared to the phase evolution diagram for normally distributed orientations in Figure 11. The phase evolution diagram (normally distributed orientation imposed) predicts alignment within the concentration regime where the phase diagram (uniformly distributed orientations imposed) predicts random orientations (isotropic phase). This is consistent with results comparing distribution shapes in the following paper[62]; given a configuration with uniform orientation distribution and a corresponding configuration with normally distributed orientations adjusted such that both configurations have identical orientational entropy, the system with normally distributed orientations is found to have higher combinatoric entropy, and therefore lower total free energy than the system with uniform orientation distribution. This means that a system of rods having uniformly distributed orientations would spontaneously rearrange into a configuration having normally distributed orientations, *given that these were the only allowed distribution shapes.*

According to the Landau-deGennes phenomenological description of the I-N transition,[77] this transition should always be first-order (discontinuous). While text books typically develop the Landau-deGennes description for three dimensions, with composition constant and temperature variable, it would remain valid for a system restricted to two dimensions, and in which temperature was constant and composition variable.[67] Thus, neither the assumption of athermal conditions nor the restriction to two dimensions in our system accounts for the observation that the order of the I-N transition depends on the type of orientation distribution imposed on the anisotropic phase. However, the Landau-deGennes description couples free energy and order parameter without specifying any particular form for the orientation distribution function. In contrast, the DLM and CMC approaches each assume a given type of distribution, allowing only the width and not the overall form to vary. While the normal distribution imposed in the CMC model is intuitively and physically more realistic than the uniform distribution assumed in Flory's original work, the dependence of order of transition on distribution type indicates the limitation of assuming that any one form of distribution persists across the entire range of concentrations covered by the calculations.

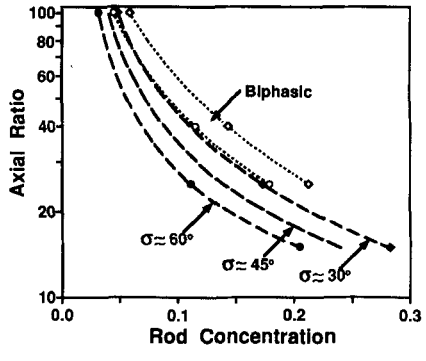

FIGURE 11 Phase diagram for rods with uniform orientation distributions imposed (dotted phase boundaries, first-order transition) compared to phase evolution diagram for rods with normally distributed orientations imposed (dashed order parameter contour lines, continuous I-N transition).

CONCLUSIONS

In conclusion, we have developed a continuum Monte Carlo (CMC) method that measures the entropy of configurations having pre-set global orientation distributions through a range of concentrations, independently of whether these configurations represent equilibrium conditions. The phases that are expected to be present at equilibrium are then determined by comparing free energy curves.

The CMC method was applied to two-dimensional, monodisperse, athermal systems and the results demonstrated that choice of the shape of the global orientation distribution can result in shifting from a first order to a continuous phase transition.

The new CMC method could be used to measure the entropies of complex orientation distributions and polydisperse systems, although such investigations are not included in the present work. Note that results presented in the following paper[62] indicate that application of CMC to polydisperse systems may be fruitful. In addition, CMC can easily examine pretransitional microstructures in the isotropic phase, as is discussed elsewhere.[63]

Acknowledgment

The authors wish to thank Pacific Northwest Laboratory, ACS-PRF (no. 21300-G7) and the I.B.M. corporation for financial support, and Prof. Bruce E. Eichinger for illuminating discussions.

References

1. H. Zocher, *Z. Anorg. Chem.*, **147**, 91 (1925).
2. H. Freundlich, *J. Phys. Chem.*, **41**(9), 1151 (1937).
3. J. H. L. Watson, W. Heller and W. Wojtowicz, *Science*, **109**, 274 (1949).
4. G. Oster, *J. Gen. Physiol.*, **33**(5), 445 (1950).
5. P. G. de Gennes, *The Physics of Liquid Crystals*, Clarendon, Oxford (1974).
6. I. Langmuir, *J. Chem. Phys.*, **6**, 873 (1938).
7. W. Maier and A. Saupe, *Z. Naturf. A*, **13**, 564 (1958).
8. P. J. Flory and G. Ronca, *Mol. Cryst. Liq. Cryst.*, **54**, 289 (1979).
9. M. Warner, *Mol. Cryst. Liq. Cryst.*, **80**, 79 (1982).
10. W. R. Romanko and S. H. Carr, *Macromolecules*, **21**, 2243 (1988).
11. J. A. Cuesta and D. Frenkel, *Phys. Rev. A*, **42**(4), 2126 (1990).
12. A. M. Somoza and P. Tarazona, *Phys. Rev. Let.*, **61**(22), 2566 (1988).
13. L. Onsager, *Ann. N. Y. Acdmy. Sci.*, **51**, 627 (1949).
14. P. J. Flory, *Proc. Roy. Soc. London A*, **234**, 73 (1956).
15. A. Isihara, *J. Chem. Phys.*, **18**, 1446 (1950).
16. A. Isihara, *J. Chem. Phys.*, **19**, 1142 (1951).
17. G. Lasher, *J. Chem. Phys.*, **53**(11), 4141 (1970).
18. J. P. Straley, *Phys. Rev. A*, **4**(2), 675 (1971).
19. J. P. Straley, *Mol. Cryst. Liq. Cryst.*, **22**, 333 (1973).
20. J. Vieillard-Baron, *J. Chem. Phys.*, **56**(10), 4729 (1972).
21. P. Sheng, *Introduction to Liquid Crystals*, Plenum Press, New York (1976).
22. R. F. Kayser and H. J. Raveche, *Phys. Rev. A*, **17**(6), 2067 (1978).
23. B. Barboy and W. M. Gelbart, *J. Chem. Phys.*, **71**(7), 3053 (1979).
24. J. Tobochnik and G. V. Chester, *Phys. Rev. A*, **27**(2), 1221 (1983).
25. H. N. W. Lekkerkerker, P. Coulon, R. Van Der Haegen, and R. Deblieck, *J. Chem. Phys.*, **80**(7), 3427 (1984).

26. U. P. Singh and Y. Singh, *Phys. Rev. A*, **33**(4), 2725 (1986).
27. M. Baus, J. L. Colot, X. G. Wu, and H. Xu, *Phys. Rev. Let.*, **59**(19), 2184 (1987).
28. J. L. Colot, X. G. Wu, H. Xu, and M. Baus, *Phys. Rev. A*, **38**(4), 2022 (1988).
29. J. A. Cuesta, C. F. Tejero, and M. Baus, *Phys. Rev. A*, **39**(12), 6498 (1989).
30. D. Frenkel and R. Eppenga, *Phys. Rev. A*, **31**(3), 1776 (1985).
31. A. Stroobants, H. N. W. Lekkerkerker, and D. Frenkel, *Phys. Rev. Lett.*, **57**(12), 1452 (1986).
32. A. Stroobants, H. N. W. Lekkerkerker, and D. Frenkel, *Phys. Rev. A*, **36**(6), 2929 (1987).
33. D. Frenkel, *J. Chem. Phys.*, **91**(19), 4912 (1987).
34. D. Frenkel, *J. Chem. Phys.*, **92**(11), 3280 (1988).
35. J. A. C. Veerman and D. Frenkel, *Phys. Rev. A*, **41**(6), 3237 (1990).
36. R. Holyst and A. Poniewierski, *Mol. Phys.*, **68**(2), 381 (1989).
37. A. Poniewierski and R. Holyst, *Phys. Rev. A*, **41**(12), 6871 (1990).
38. B. Tjipto-Margo and G. T. Evans, *J. Chem. Phys.*, **93**(6), 4254 (1990).
39. E. A. DiMarzio, *J. Chem. Phys.*, **35**(2), 658 (1961).
40. M. A. Cotter and D. E. Martire, *Mol. Cryst. Liq. Cryst.*, **7**, 295 (1969).
41. M. A. Cotter and D. E. Martire, *J. Chem. Phys.*, **53**, 4500 (1970).
42. A. Wulf and A. G. DeRocco, *Liquid Crystals and Ordered Fluids*, Proc. Am. Chem. Soc. Symp. on Ordered Fluids and Liquid Crystals, Plenum Press, NY (1970).
43. R. Alben, *Mol. Cryst. Liq. Cryst.*, **13**, 193 (1971).
44. M. A. Cotter, *Mol. Cryst. Liq. Cryst.*, **35**, 33 (1976).
45. P. J. Flory and A. Abe, *Macromolecules*, **11**(6), 1119 (1978).
46. A. Abe and P. J. Flory, *Macromolecules*, **11**(6), 1122 (1978).
47. P. J. Flory and R. S. Frost, *Macromolecules*, **11**(6), 1126 (1978).
48. R. S. Frost and P. J. Flory, *Macromolecules*, **11**(6), 1134 (1978).
49. P. J. Flory and G. Ronca, *Mol. Cryst. Liq. Cryst.*, **54**, 311 (1979).
50. M. Warner and P. J. Flory, *J. Chem. Phys.*, **73**(12), 6327 (1980).
51. M. Warner, *Mol. Cryst. Liq. Cryst.*, **80**, 67 (1982).
52. J. Moscicki and G. Williams, *Polymer*, **23**, 558 (1982).
53. P. J. Flory, *Advances in Polymer Science*, **59**, 1 (1984).
54. P. A. Irvine, D. C. Wu and P. J. Flory, *Chem. Soc. Farad. Trans 1*, **80**, 1795 (1984).
55. P. J. Flory and P. A. Irvine, *Chem. Soc. Farad. Trans 1*, **80**, 1807 (1984).
56. M. G. Bawendi and K. F. Freed, *J. Chem. Phys.*, **85**(5), 3007 (1986).
57. F. Dowell, *Phys. Rev. A*, **28**(2), 1003 (1983).
58. F. Dowell, *Phys. Rev. A*, **28**(6), 3520 (1983).
59. F. Dowell, *Phys. Rev. A*, **28**(6), 3526 (1983).
60. F. Dowell, *J. Chem. Phys.*, **91**(2), 1316 (1989).
61. F. Dowell, *J. Chem. Phys.*, **91**(2), 1326 (1989).
62. L. A. Chick and C. Viney, *Mol. Cryst. Liq. Cryst.*, **226**, 41 (1993).
63. L. A. Chick and C. Viney, *Mol. Cryst. Liq. Cryst.*, **226**, 63 (1993).
64. H. Okamoto, *J. Chem. Phys.*, **64**(6), 2686 (1976).
65. L. A. Chick, C. Viney, and I. A. Aksay, *Processing Science of Advanced Ceramics, Mtrl. Res. Soc. Symp. Proc. Vol. 155*, ed. by I. A. Aksay, G. L. McVay, and D. R. Ulrich, Mtrl. Res. Soc., Pittsburgh, Pennsylvania, 331 (1989).
66. P. Yager, P. E. Schoen, C. Davies, R. Price, and A. Singh, *Biophysical J.*, **48**, 899 (1985).
67. L. D. Landau and E. M. Lifshitz, *Statistical Physics*, Pergamon, London (1958).
68. J. M. Kosterlitz and D. J. Thouless, *J. Phys. C*, **6**, 1181 (1973).
69. D. H. Van Winkle and N. A. Clark, *Phys. Rev. A*, **38**(3), 1573 (1988).
70. L. A. Chick, *Ph.D. Dissertation*, University of Washington (1990). (Available through University Microfilms, 300 North Zeeb Road, Ann Arbor, Michigan 48106.)
71. D. Y. Yoon and A. Baumgartner, *Macromolecules*, **17**(12), 2864 (1984).
72. A. Baumgartner, *J. Chem. Phys.*, **84**(3), 1905 (1986).
73. J. H. van Vliet and G. ten Brinke, *Macromolecules*, **22**, 4627 (1989).
74. J. P. Downey and J. Kovac, *Macromolecules*, **23**(11), 3013 (1990).
75. B. Widom, *J. Chem. Phys.*, **39**(11), 2808 (1963).
76. P. Gordon, *Principles of Phase Diagrams in Materials Systems*, McGraw-Hill, New York (1968).
77. G. Vertogen and W. H. deJeu, *Thermotropic Liquid Crystals, Fundamentals*, Springer Verlag, Berlin (1988), Chapter 12.